International Geology Review

ISSN: (Print) (Online) Journal homepage: https://www.tandfonline.com/loi/tigr20

Zircon xenocrysts in Late Cretaceous magmatic rocks in the Kermanshah Ophiolite: link to Iran continental crust supports the subduction initiation model

H.S. Moghadam, Q.L. Li, R.J. Stern, W.L. Griffin & S.Y. O'Reilly

To cite this article: H.S. Moghadam, Q.L. Li, R.J. Stern, W.L. Griffin & S.Y. O'Reilly (2022) Zircon xenocrysts in Late Cretaceous magmatic rocks in the Kermanshah Ophiolite: link to Iran continental crust supports the subduction initiation model, International Geology Review, 64:22, 3248-3259, DOI: 10.1080/00206814.2022.2043193

To link to this article: https://doi.org/10.1080/00206814.2022.2043193

INTERNATIONAL GEOLOGY REVIEW
2022, VOL. 64, NO. 22, 3248–3259
https://doi.org/10.1080/00206814.2022.2043193

Taylor & Francis
Taylor & Francis Group

Zircon xenocrysts in Late Cretaceous magmatic rocks in the Kermanshah Ophiolite: link to Iran continental crust supports the subduction initiation model

H.S. Moghadam[a,b,c], Q.L. Li[c], R.J. Stern[d], W.L. Griffin[b] and S.Y. O'Reilly[b]

[a]School of Earth Sciences, Damghan University, Damghan Iran; [b]Ccfs and Gemoc Arc National Key Centre, Macquarie University, Sydney, New South Wales Australia; [c]Institute of Geology and Geophysics, Chinese Academy of Sciences, Beijing, People Rebublic's of china, China; [d]Geosciences Department, University of Texas at Dallas, Richardson, Tx USA

ABSTRACT

Geochronological and geochemical data show that Late Cretaceous Zagros ophiolites were generated by forearc seafloor spreading during a subduction initiation event along the southwestern margin of Iran. These ophiolites define a ~ 3000 km long belt passing from Cyprus to Turkey, Syria, Iran, the UAE, and Oman. Ten samples of plagiogranites, amphibole gabbros and diorites of the Kermanshah ophiolite yield U-Pb zircon magmatic ages indicating ophiolite formation at 98 to 96 Ma. Some Kermanshah rocks also contain abundant zircon xenocrysts with age peaks (in order of decreasing size): Triassic (~247 Ma), mid-Paleoproterozoic (~2150 Ma), Late Paleoproterozoic (~1850 Ma), Late Ediacaran (~560 Ma), Early Cretaceous (~140 Ma), and Tonian (~850 Ma). Similar age peaks are seen in magmatic and detrital rocks of Iranian crust to the north. The xenocrysts have εHf(t) values from +6.3 to – 21.6, corresponding to depleted mantle Hf model ages (T_{DM}) of 0.6 to 3.6 Ga. The xenocryst age peaks are similar to those of zircons in Iranian continental crust. The occurrence of zircon xenocrysts in the Kermanshah ophiolite suggests that this formed adjacent to the Iranian continent, as expected for Late Cretaceous subduction initiation.

ARTICLE HISTORY
Received 2 November 2021
Accepted 31 January 2022

KEYWORDS
Zircon; U-pb geochronology; plagiogranite; zagros ophiolites; Iran

1. Introduction

Ophiolites are key indicators of plate tectonics, but it is often uncertain where they formed relative to the crust that they are emplaced upon. Some ophiolites are thought to form far out in an ocean basin (allochthonous) and other ophiolites may have formed very near to where they are emplaced (para-autochthonous) (e.g. Searle and Malpas 1980; Whetten *et al*. 1980; Savelieva *et al*. 1997). Further controversy swirls around increasing interpretations that most ophiolites form as upper-plate responses to subduction initiation (e.g. Stern *et al*. 2012; Stern and Gerya 2018), especially supra-subduction zone (SSZ) ophiolites. The Bitlis-Zagros ophiolites of Turkey and Iran, part of the most extensive and best-studied SSZ-type Neotethyan ophiolite belt in the world, are increasingly accepted to have formed in response to a Late Cretaceous SI event on the southern margin of Eurasia (Moghadam and Stern 2011). A key test of this hypothesis is demonstrating that these ophiolites formed near the older continental crust of Turkey and Iran. This paper reports the first evidence for zircon xenocrysts in plutonic rocks of an excellent example of Zagros ophiolites, the Kermanshah ophiolite of NW Iran. The first zircon U-Pb ages for the magmatic rocks from the Kermanshah ophiolites were reported by Ao *et al*. (2016) and Nouri *et al*. (2016).

The philosophy of this study is that because SI ophiolites that form by a passive margin or transform margin collapse adjacent to continents are para-autochthonous (e.g. Stern and Bloomer 1992), they might be expected to contain zircon xenocrysts that reflect those in the nearby continental crust. If they do not – or if they contain zircon xenocrysts with a different age spectrum – then the SI interpretation is weakened. If they do, then the SI interpretation is supported. This study uses the excellent Late Cretaceous ophiolite near Kermanshah in SW Iran for this purpose. Our results show that the Kermanshah ophiolite formed next to Iranian continental crust and is para-autochthonous, supporting the SI model for the origin of Late Cretaceous Bitlis-Zagros ophiolites.

2. Regional geology

Late Cretaceous ophiolites can be traced for more than 3000 km along the SW margin of Eurasia, from Cyprus (Troodos) through SE Turkey, NW Syria, NE Iraq, SW Iran,

CONTACT H.S. Moghadam hadishafaii@du.ac.ir Damghan University, Damghan Iran
This article has been corrected with minor changes. These changes do not impact the academic content of the article.

NE UAE and northern Oman. Recent geochemical and geochronological studies of these ophiolites show a temporal evolution in the volcanic sequence from mid-ocean ridge basalt (MORB)-like tholeiitic magmas to arc tholeiites, calc-alkaline and boninitic suites; OIB-like suites are also found (e.g. (Ishikawa *et al*. 2002; Moghadam and Stern 2011, 2015; Dilek and Furnes 2014; Monsef *et al*. 2014, 2019)). Geochronological and geochemical data indicate that Bitlis-Zagros-Oman ophiolites formed in a forearc spreading system during ~8 Myr between *ca* 100 and 92 Ma (Warren *et al*. 2005; Rioux *et al*. 2013, 2016; Dilek and Furnes 2014; Monsef *et al*. 2018; Furnes *et al*. 2020), as expected for SI-related ophiolites (Stern *et al*. 2012).

Late Cretaceous Zagros ophiolites in southwestern Iran lie along the main Zagros Thrust (MZT, Figure 1A) and include, from NW to SE: Kermanshah, Neyriz and Haji-Abad ophiolites. Zagros ophiolites have mantle and crustal sequences with SSZ-type geochemical signatures, i.e. depletion in Nb-Ta and enrichment in large-ion lithophile elements and light rare earth elements in magmatic rocks and high Cr# (100 Cr/Cr+Al) in mantle peridotite spinels (Moghadam and Stern 2011). Zagros ophiolites and other Late Cretaceous ophiolites along the Bitlis-Zagros suture zone including the Oman and Mediterranean ophiolites are suggested to have formed during subduction initiation in a forearc setting (Moghadam and Stern 2011, 2015; Dilek and Furnes 2014; Monsef *et al*. 2018). Recent zircon U-Pb ages show that the Zagros forearc magmatism occurred during 105 to 94 Ma (Middle-Late Cretaceous) (Moghadam *et al*. 2021b).

The Kermanshah ophiolite encompasses ~2400 km^2. It is thrust over a thick Permian-Triassic sequence of pelagic limestones (Bisotun limestones), radiolarites, ocean Island basalt (OIB), enriched mid-

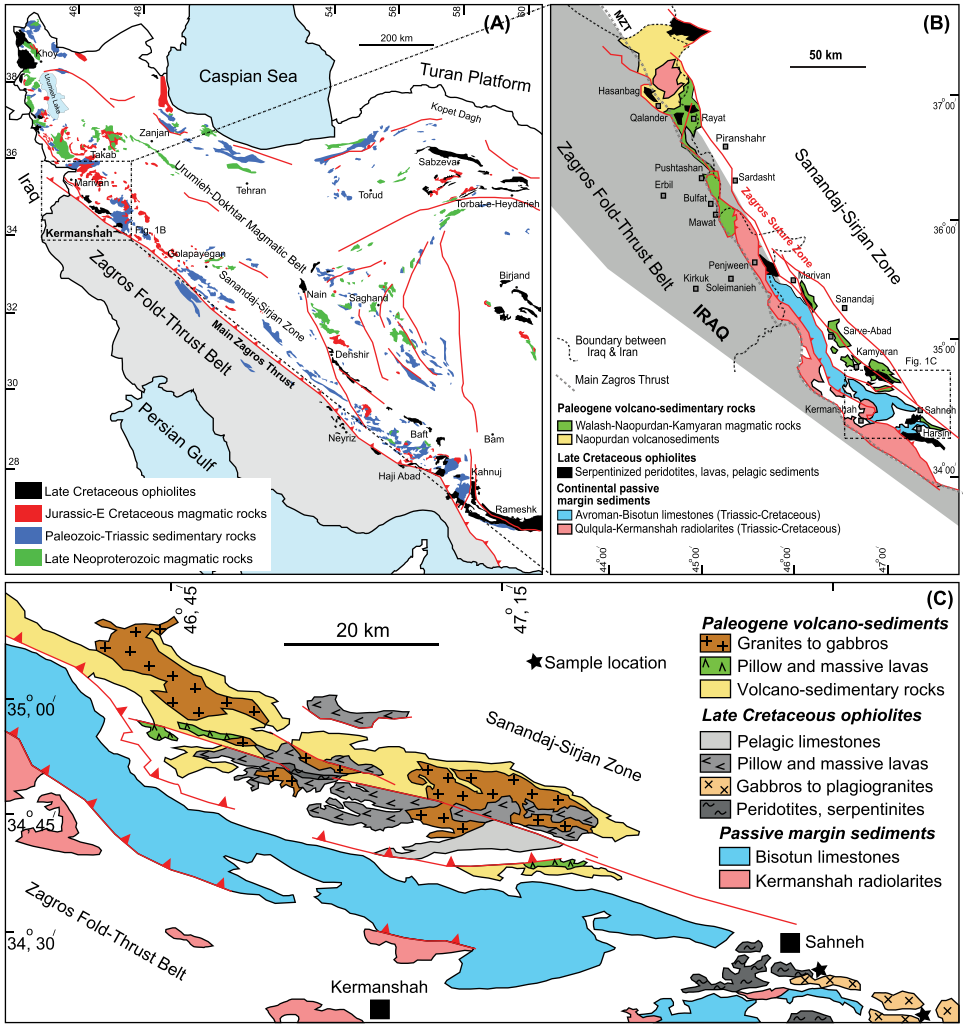

Figure 1. (A) geological map of Iran showing late cretaceous ophiolites and phanerozoic-late neoproterozoic magmatic and sedimentary rocks which could be the source of zircon xenocrysts in kermanshah ophiolitic rocks. (b) simplified map showing the distribution of late cretaceous forearc ophiolites and palaeogene oceanic rocks (walash- naopurdan-kamyran series) along the Iran-Iraq border (modified after (Ali *et al*. 2013)). (c) geological map of late cretaceous ophiolites, palaeogene magmatic and sedimentary sequences and triassic-cretaceous passive margin sedimentary rocks in the kermanshah region.

ocean-ridge basalts (E-MORB-like), and minor felsic intrusive and extrusive rocks that are geochronologically and geochemically similar to Triassic (*ca* 230 Ma) alkaline igneous rocks of the Hawasina Nappes of Oman (Chauvet *et al*. 2011; Saccani *et al*. 2013) (Figures 1B). Uplift of the Kermanshah ophiolite occurred before or during Maastrichtian-Palaeocene time, as evidenced by ophiolitic clasts in the Maastrichtian-Palaeocene Amiran Conglomerate Formation of the Zagros Fold-Thrust Belt. Formation of the Permo-Triassic sedimentary sequence was related to Gondwana rifting and opening of Neotethys. Following rifting, the SW margin of Iran was a passive margin until Late Cretaceous subduction initiation (Wrobel-Daveau *et al*. 2010; Azizi and Stern 2019). The Kermanshah ophiolite has a mostly faulted contact with Triassic chlorite-epidote schists, greywackes, and metavolcanic rocks of the Sanandaj-Sirjan zone (Agard *et al*. 2005). The ophiolite is also in contact with Jurassic Hamadan phyllites and sandstones (Braud and Bellon 1974). In some places, the contact between the Kermanshah ophiolite and Sanandaj-Sirjan zone rocks is covered by Palaeogene volcanic-sedimentary rocks of the Walash-Naopurdan-Kamyaran unit (Figure 1B).

The Late Cretaceous Kermanshah ophiolite comprises mantle peridotites, flaser gabbros, coarse-grained (olivine-bearing) gabbros, diorites and amphibole gabbros, minor tonalites and trondhjemites ('plagiogranites'), pillowed and massive lavas and overlying sediments (Fig. S1). Cumulate gabbros also occur as ~5–10 m magmatic pockets intruding mantle peridotites. Mantle peridotites include harzburgite, depleted lherzolite and pervasively impregnated harzburgite. The crustal sequence contains both fine- to coarse-grained cumulate amphibole gabbros-diorites and highly deformed ultramafic (wehrlite to lherzolite)-gabbroic rocks. Plagiogranites are injected into crustal gabbros and diorites and within the serpentinized mantle peridotites.

Volcanic rocks comprise basaltic lava flows and pillow basalts, capped by and/or interlayered with Turonian-Maastrichtian (93–65 Ma) pelagic limestones. These volcanic rocks, along with intrusive rocks such as gabbros and diorites, have both arc-tholeiitic and calc-alkaline geochemical signatures, attesting to their formation in a SSZ-related setting (Moghadam and Stern 2011). The ophiolite is covered and/or intruded by Cenozoic volcano-sedimentary rocks, basaltic to andesitic lavas and granitoids.

3. Field geology and sample descriptions

Kermanshah plagiogranites occur south of Sahneh, mostly near the Siah-Chogha village, but also occur east of Harsin and in Gamasyab (Figure 1). Plagiogranites mostly occur as 10->20 m pockets with melano-gabbros, both in contact with serpentinized peridotites. In addition, foliated leucogabbros, melanogabbros and lherzolites occur at the contact with plagiogranites in Sahneh. All of these rocks are in faulted contact with Bisotun limestones and Kermanshah radiolarites to the west, but to the east plagiogranites are covered by Pleistocene alluvium. Rootless plagiogranites mixed with other rocks as a tectonic melange also occur around the Gamasyab river. Plagiogranites are fine to coarse-grained and contain variably altered (clay minerals and sericite) plagioclase phenocrysts (Figure 2). Anhedral quartz occurs between plagioclases. Alkali-feldspar (orthoclase) occupies less than 10%. Chloritized hornblendes are also common in these rocks. Other secondary minerals include chlorite, epidote and calcite.

Our analysed plagiogranites (three samples) contain SiO_2 = 60.5–71.9 wt.%, K_2O = 0.07–0.24 and Na_2O = 1.6–5.7 wt.% (Table S1). Compositionally, they have dioritic to tonalitic-granitic compositions. In a chondrite-normalized diagram, they have flat REE patterns with $La_{(n)}/Yb_{(n)}$~1.3, with slight depletion or enrichment in Eu (Figure 3). These rocks also show depletion in Nb, Ta and Ti and enrichment in large ion lithophile elements. Except for depletion in Ti due to the fractionation of Ti-rich oxides, the trace elements patterns of plagiogranites are similar to tholeiitic basalts from the Kermanshah ophiolites (Figure 3).

4. Analytical procedures

In this paper, we present U-Pb ages and Lu-Hf isotopic analyses of zircons from 7 Kermanshah ophiolite samples which contain mostly xenocrystic zircons. We used ages for four other plagiogranite samples with only magmatic zircons presented in another paper that deals with age and trace element-isotope geochemistry of all Zagros ophiolites including Kermanshah and Neyriz (Moghadam *et al*. 2021b) to emphasize Zagros ophiolite crystallization ages and the formation of oceanic forearc crust (Fig. S2). We used two methods for separating zircons to avoid laboratory contamination. These include conventional crushing, sieving, heavy liquids and handpicking and an innovative technique based on Selfrag, which uses high-voltage electric discharges to disaggregate rocks without any risk of contamination. Prior to U-Pb analysis, all zircons

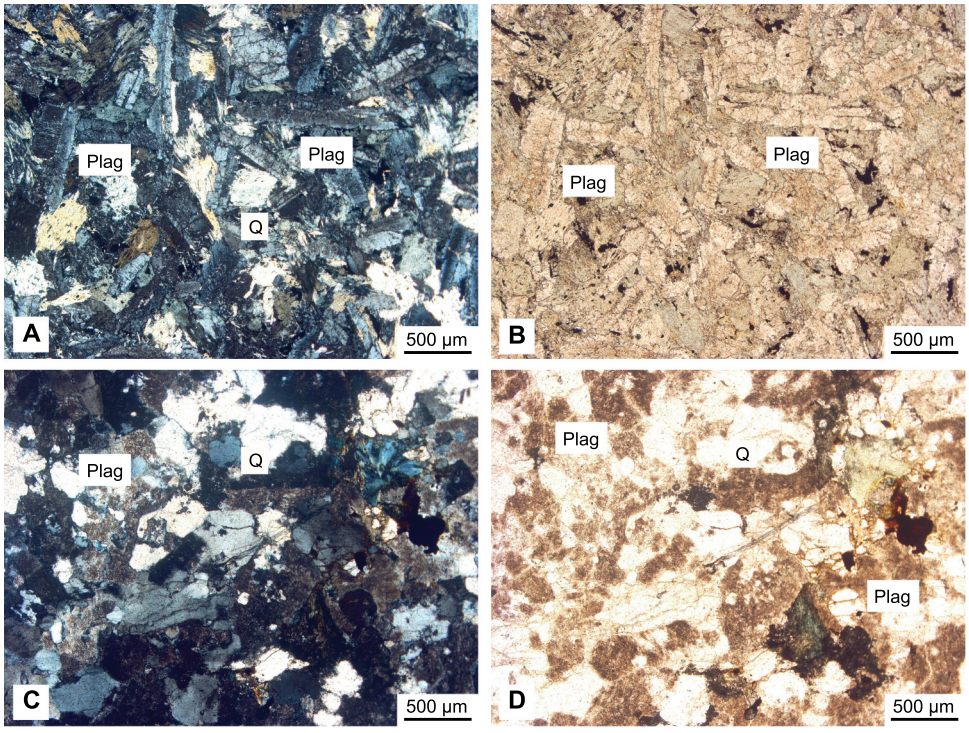

Figure 2. Thin-section microphotographs showing the mineralogical composition of kermanshah ophiolite plagiogranites. abbreviation; q = quartz and plag = plagioclase. chloritized amphiboles are in the centre and left of a and b. left photos are cross-polarized light, whereas right photos are plane-polarized light.

were imaged by Cathodoluminescence (CL) to examine their internal structure. CL images were obtained using a Scanning Electron Microscopes at CCFS, Macquarie University (Australia) and at the Institute of Geology and Geophysics, Chinese Academy of Sciences (IGG-CAS, Beijing).

Zircon U-Pb dating was carried out using both Cameca IMS-1280/HR Secondary Ion Mass Spectrometry (SIMS) at IGG-CAS and Laser Ablation Inductively Coupled Plasma-Mass Spectrometry (LA-ICP-MS) at CCFS. Zircons were further analysed for Lu-Hf isotopes using a laser ablation microprobe attached to a multicollector-inductively coupled plasma-mass spectrometer at IGG-CAS. Detailed analytical methods are given in Supplementary Document A.

5. Results

We carried out zircon U-Pb geochronology on four plagiogranites (samples KR14-32B, KR14-27, KR14-33A and KR14-33B), one amphibole gabbro (sample KR14-29B), one diorite (sample KR14-28B) and one highly deformed (mylonitic) gabbro, all from the Kermanshah ophiolite crustal sequence. We tried to separate zircons from several mylonitic gabbros, but only one sample contained a few (n = 3) grains with ages of *ca* 0.5 to 2.5 Ga, which we have ignored for purposes of calculating magmatic ages. Plagiogranites analysed by Moghadam *et al.* (2021b) contain only Late Cretaceous magmatic zircons with 99.5 to 96 Ma ages: 96.1 ± 0.2 Ma (sample KR14-30B), 97.8 ± 0.9 Ma (sample KR14-30), 98.1 ± 0.2 Ma (sample KR19-29) and 99.5 ± 0.2 Ma (sample KR14-28A) (Fig. S2). These are slightly older but overlap with zircon (95.0 ± 2.4 Ma) and baddeleyite (94.6 ± 2.7 Ma) ages reported by Nouri *et al.* (2016). These also agree with microfossil ages obtained from pelagic sediments intercalated with Kermanshah pillow lavas and are comparable with zircon U-Pb ages of other Zagros ophiolites such as Neyriz. These ages indicate when Zagros ophiolites formed (Moghadam and Stern 2011; Monsef *et al.* 2018). Some samples (e.g. plagiogranites KR14-32B and KR14-27) contain both old zircon xenocrysts and a few Late Cretaceous zircons.

Zircons handpicked from the Kermanshah ophiolitic rocks vary in shape from euhedral (elongated to equant) to rounded, and in some cases have convolute or oscillatory zoning or are unzoned (Fig. S3). Most old zircons (>2 Ga) are unzoned or show convolute zonation, and some are rounded. Some xenocryst zircons show rims (Fig. S3A), but these are too thin for U-Pb analysis. Energy Dispersive Spectroscopy (EDS-SEM) analyses reveal that some inherited zircons host mineral inclusions such as apatite, feldspar, quartz and titanomagnetite; no high-pressure minerals were detected.

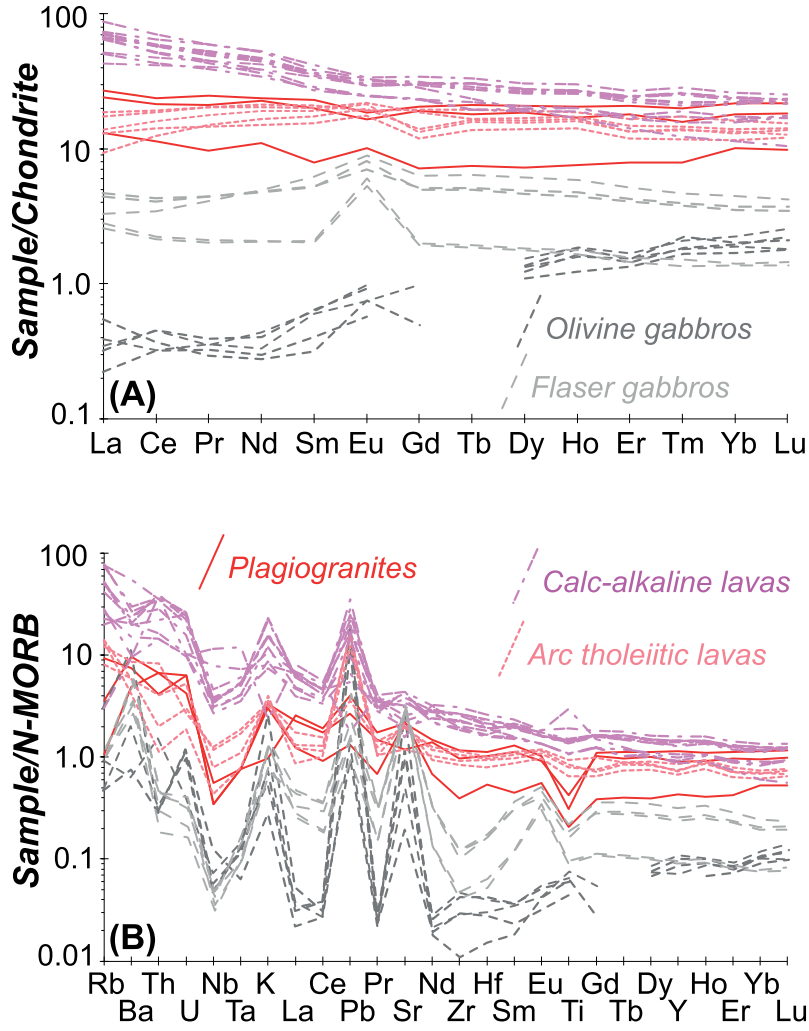

Figure 3. Chondrite-normalized REE patterns (chondritic abundances from (mcdonough and sun 1995)) and primitive-mantle and n-morb-normalized multi-element patterns (n-morb and primary mantle concentrations from (mcdonough and sun 1995)) for kermanshah plagiogranites. geochemical data for kermanshah gabbros and lavas are from (moghadam *et al.* 2021b).

SIMS and LA-ICP-MS analyses of zircons from plagiogranites, diorites and amphibole gabbros yield old U-Pb ages (in addition to 6 grains with Late Cretaceous ages of 104 to 96 Ma; see Tables S2 to S3) interpreted as xenocrysts: Early Cretaceous (135–123 Ma, 5 grains), Jurassic-Early Triassic (250–155 Ma, 16 grains), Permian (290–255 Ma, 8 grains), Carboniferous-Devonian (421–312 Ma, 5 grains), Cadomian (625–526 Ma, 7 grains), Cryogenian-Tonian (929–652 Ma, 8 grains), Mesoproterozoic (1.5–1 Ga, 3 grains), Paleoproterozoic (2.5–1.6 Ga, 29 grains) and Meso-Archaean (~3 Ga, 1 grain). In a Kernel density estimation (KDE) plot (Figure 4A, drawn by 'isoplot R', (Vermeesch 2018)), zircon xenocrysts show main peaks at 141 (Early Cretaceous), 247 (Early Triassic), 557 (Ediacaran), 847 (Cryogenian), 1749 and 2147 Ma (Middle to Late Paleoproterozoic) (Figure 2A).

Zircon xenocrysts from Kermanshah ophiolite magmatic rocks show εHf(t) values from +6.3 to – 21.6 (Figure 4B), corresponding to depleted mantle Hf model ages (T_{DM}) of 0.6 to 3.6 Ga (Table S3). There is no systematic correlation between ages and Hf isotope values. Mesozoic zircons (Early Cretaceous to Triassic) have εHf(t) of +6.3 to – 20.5, whereas Palaeozoic zircons have εHf(t) of +5.7 to – 11.9. Cadomian zircons have εHf(t) of +1.5 to – 14.6 and Meso- to Paleoproterozoic zircons have εHf(t) of +5.6 to – 21.6.

6. Discussion

This section discusses possible mechanisms for concentrating zircon xenocrysts in the Kermanshah ophiolite. We further discuss the significance of these xenocrysts for understanding the formation of Zagros forearc ophiolites.

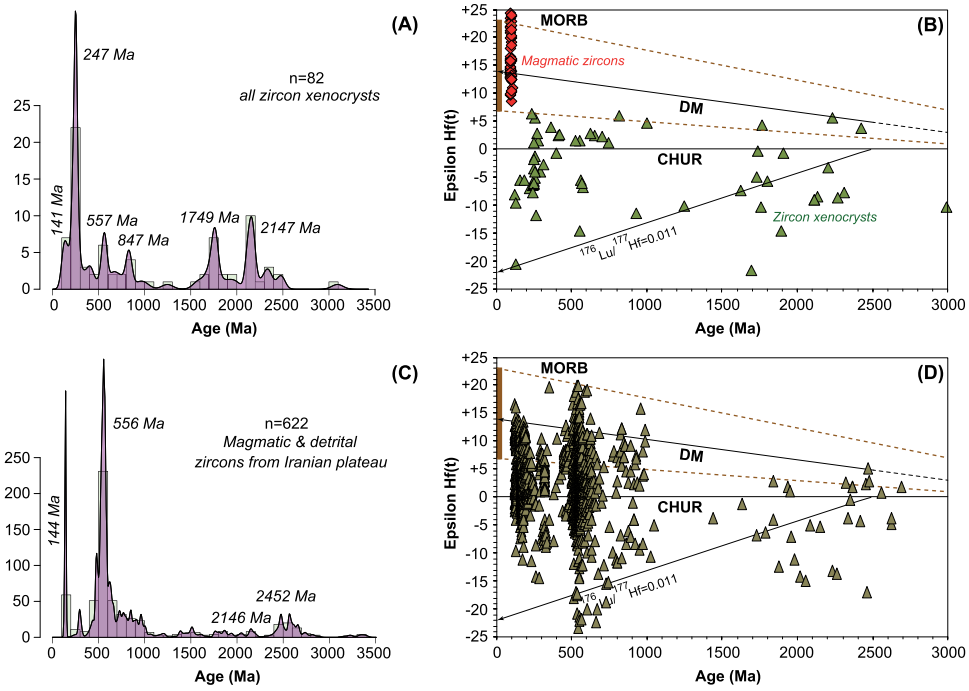

figure 4. kernel density estimation (kde) plot for zircon xenocrysts in kermanshah ophiolite magmatic rocks (a) and their hf isotopic composition *vs* zircon u/pb age (b). the composition of magmatic zircons from kermanshah plagiogranites are from moghadam et al., in press. for comparison we also show the age (c) and hf isotopic composition (d) of the magmatic and sedimentary rocks from the Iranian plateau (data from (moghadam *et al.* 2020a, 2021a)). $^{176}lu/^{177}hf$ values of 0.011 for upper continental crust is from (Griffin *et al.* 2004).

6-1. Significance of zircon xenocrysts

Zircon xenocrysts are also reported from some other ophiolites from Iran, e.g. Torbat-e-Heydarieh ophiolite in NE Iran (Figure 1A) which contains zircons as old as 1.1 to 1.5 Ga (Moghadam *et al.* 2020b) and mafic rocks from the Fanuj-Maskutan ophiolites (Makran, S Iran) with 515 Ma zircon xenocrysts (Sepidbar *et al.* 2020). Zircons from most Kermanshah ophiolite magmatic rocks yield Late Cretaceous ages, ranging from 100 to 96 Ma (Fig. S2), which are interpreted as crystallization ages (Moghadam *et al.* 2021b). These are consistent with microfossil ages of sediments overlying this ophiolite (Moghadam and Stern 2011) and with ages of other ophiolites along the Main Zagros Thrust (MZT), including the Neyriz ophiolite with zircon U-Pb ages of 100.1 ± 2.3 to 93.4 ± 1.3 Ma (Monsef *et al.* 2018). These ages are also similar to those of other ophiolites along the Bitlis-Zagros suture zone; e.g. zircon U-Pb ages of 94–90 Ma for Troodos plagiogranites (Maffione *et al.* 2017); 96–95 Ma for Samail (Oman) ophiolite gabbros and plagiogranites (Warren *et al.* 2005; Rioux *et al.* 2013, 2016) and 92–91 Ma for Kizildag plagiogranites (Dilek and Thy 2009). These Late Cretaceous ages of magmatic zircons are interpreted to date the time of crystallization and to constrain the timing of subduction initiation along the Eurasian margin, which seems to have started in the Kermanshah-Neyriz region and propagated E and W. Pre-Late Cretaceous zircon ages are considered to be inherited. Samples KR14-28B and KR14-27 also contain a few Late Cretaceous magmatic zircons in addition to xenocrysts.

The εHf(t) values for Late Cretaceous zircons range from +8.7 to +26 (Table S4), suggesting that the magmas that formed these were derived from depleted mantle sources (Moghadam *et al.* 2021b). In contrast, zircon xenocrysts have both positive and negative εHf(t). Most inherited zircons (41 of 61) have negative εHf(t) (Figure 4B), suggesting that their parental magmas are recycled from old continental crust. The age and Hf-isotope signatures of Kermanshah zircon xenocrysts are in the range of zircons from magmatic and sedimentary rocks of Iranian continental crust (4C-D).

6-2. Source of zircon xenocrysts

Magmatic rocks from other ophiolites around the world contain inherited zircons (e.g. Peltonen *et al.* 2003; Whattam *et al.* 2006; Smyth *et al.* 2007; Rojas-Agramonte *et al.* 2016a; Torró *et al.* 2018; Proenza *et al.* 2018a; Lian *et al.* 2020). Three main mechanisms have been suggested for incorporating old zircons in ophiolite magmas: (a) from subduction zones, (b) from old

sub-continental lithospheric mantle (SCLM), and (c) from assimilation of continental crust and/or upper crust sediments. Mechanism (a) may occur in mature magmatic arcs to produce arc magmas, mostly in rocks with radiogenic Pb and Sr and non-radiogenic Hf isotopic compositions. Mechanism (b) could provide zircons with positive εHf(t) values from refertilized mantle. Mechanism (c) is likely where magmas interact with upper continental crust and sediments and could form zircons with variable εHf(t) values. These possibilities are explored further below.

Old zircon xenocrysts may have been introduced into the shallow mantle wedge by subducting detrital sediments deposited on the seafloor near the trench and/or by subduction erosion of forearc continental crust (Yamamoto *et al*. 2013b; Rojas-Agramonte *et al*. 2016b). Most evidence for such recycling relies on the isotopic composition of convergent margin lava. Zircon, because of its exceptional physical and chemical strength is the most notable possible exception (Harley *et al*. 2007; Bindeman and Melnik 2016). The best evidence that zircons can be recycled through subduction zones is the presence of xenocrystic zircons in some intra-oceanic arc basalts (Rojas-Agramonte *et al*. 2016a).

The first possibility is that the inherited zircons were transported into the mantle beneath the Kermanshah forearc as detrital grains in sediments on top of the subducting Neotethyan oceanic slab and hence to the region of melt generation by diapirs (e.g. Marschall and Schumacher 2012; Spandler and Pirard 2013; Rojas-Agramonte *et al*. 2016b; Proenza *et al*. 2018b), ultimately to be incorporated into ophiolite magmas. This interpretation is supported by Sr-Nd-Pb isotope results for the Kermanshah ophiolite which emphasized the role of subducted sediments in magmagenesis (Moghadam *et al*. 2021b). However, zircons recycled through subduction would have to reside in the hot mantle wedge without significant resetting of their U-Pb ages before being entrained into magmatic rocks (Stern *et al*. 2010). Although, empirical evidence shows that zircon can stay in the shallow upper mantle for extended periods of time (even >1 Ga) (Rojas-Agramonte *et al*. 2021), but considering how subducted components are transported up into the mantle wedge and the likelihood of zircon dissolution or resetting, it seems unlikely that xenocrysts could be transported and recycled into the shallow oceanic mantle without resetting. There are other, similar explanations including, recycling of older crustal materials from the deep mantle introduced by previous subduction processes, and zircon entrapment by a mantle plume (Yang *et al*. 2015). The best evidence for this assumption is the presence of zircon xenocrysts in ophiolitic peridotites and chromitites (Yamamoto *et al*. 2013a; McGowan *et al*. 2015; Griffin *et al*. 2016; Lian *et al*. 2020). The other alternative is transport via aborted thermo-chemical diapirs which can be incorporated into the shallow mantle (*ca* 50 km deep; (Blanco-Quintero *et al*. 2011; Rojas-Agramonte *et al*. 2016b; Proenza *et al*. 2018b). This mechanism is similar to mechanism (a), i.e. sediment subduction into the mantle wedge, as described above. Such diapirs can include partially molten hydrated peridotite, dry solid mantle rocks, and subducted oceanic crust and sediments (Gorczyk *et al*. 2007a; Blanco-Quintero *et al*. 2011), which may include zircon-bearing detrital sediments. Ascent of these plumes from >100 km depth brings asthenosphere and lithospheric mantle and subducted crustal materials to shallow mantle depths, where it could contribute to arc magmatism (Gorczyk *et al*. 2007b).

The second possibility for Kermanshah old zircons is that these are inherited from Iranian sub-continental lithospheric mantle (SCLM), similar to the proposed mechanism for incorporating inherited zircons in Arabian-Nubian Shield mafic rocks (Stern *et al*. 2010). About one-third of the zircon xenocrysts from the Kermanshah ophiolites (20 of 61 grains) have positive εHf(t) values (Table S4), typical of zircon that crystallized from melts derived from a juvenile SSZ-related source. These zircons could originally have crystallized within ancient SCLM. Isotopic and trace element ratios such as Nb/Yb show that some Kermanshah ophiolite magmatic rocks were derived from an enriched mantle source, i.e. possibly ancient SCLM and this could have also provided the old zircons.

The third possibility is that zircon xenocrysts are products of magmatic assimilation of Iranian continental crust and sediments. Xenocrysts show a pattern of ages and Hf-isotopic compositions that broadly resembles zircons in older magmatic and sedimentary rocks of Iran to the N and NE. Jurassic to Early Cretaceous magmatic rocks are abundant in the Sanandaj-Sirjan zone and are interpreted to have formed during rifting of Iranian continental lithosphere with significant contamination by upper crust and sediments (Azizi and Stern 2019). This process can produce magmatic rocks with variable Hf-isotope compositions, similar to those found as xenocrysts in Kermanshah rocks. Triassic, Permian to Carboniferous and Devonian rocks are rare in the Sanandaj-Sirjan zone but there are granitic rocks in the region with these ages (e.g. Honarmand *et al*. 2017; Moghadam *et al*. 2020a), which could have supplied zircon xenocrysts in the Kermanshah rocks. Sedimentary successions as well as metamorphic rocks with pelitic to psammitic protoliths such as Triassic and Jurassic schists, phyllites, greywackes and sandstones

from the Sanandaj-Sirjan zone can also considered as the source for Triassic, Permian to Carboniferous detrital zircons. The abundance of detrital zircons in clastic sediments can vary tremendously, depending on the 'fertility' of unroofed bed rocks (Malusà *et al*. 2016). Cadomian and older zircons can be supplied from Cadomian magmatic and sedimentary rocks which are widespread in Iranian crust to the north (Moghadam *et al*. 2021a). We prefer the third explanation because this is most consistent with the observation that xenocrysts are especially common in Kermanshah felsic rocks.

Our data suggest that zircon xenocrysts were supplied from Iranian passive margin sediments (Figure 5). The common occurrence of Mesozoic, Palaeozoic and Cadomian rocks containing Early Cretaceous to Paleoproterozoic zircon from the Iranian continental margin, with similar age peaks in the KDE plot (Figure 4C) and identical εHf(t) values (Figure 4D) supports the interpretation that zircon xenocrysts survived partial melting of Iranian continental margin sediments during mafic igneous activity associated with subduction initiation to form the Zagros ophiolites. It is especially noteworthy that no pre-Ediacaran crust is known in Iran, so older xenocrysts must be recycled from sedimentary rocks. This interpretation is supported by the observation that old xenocrysts (>2 Ga) are well-rounded, suggesting mechanical abrasion during sedimentary transport.

The abundance of xenocrystic zircons in plagiogranites and other felsic rocks of the Kermanshah ophiolite indicates the importance of understanding how these magmas formed. Scenarios proposed for forming

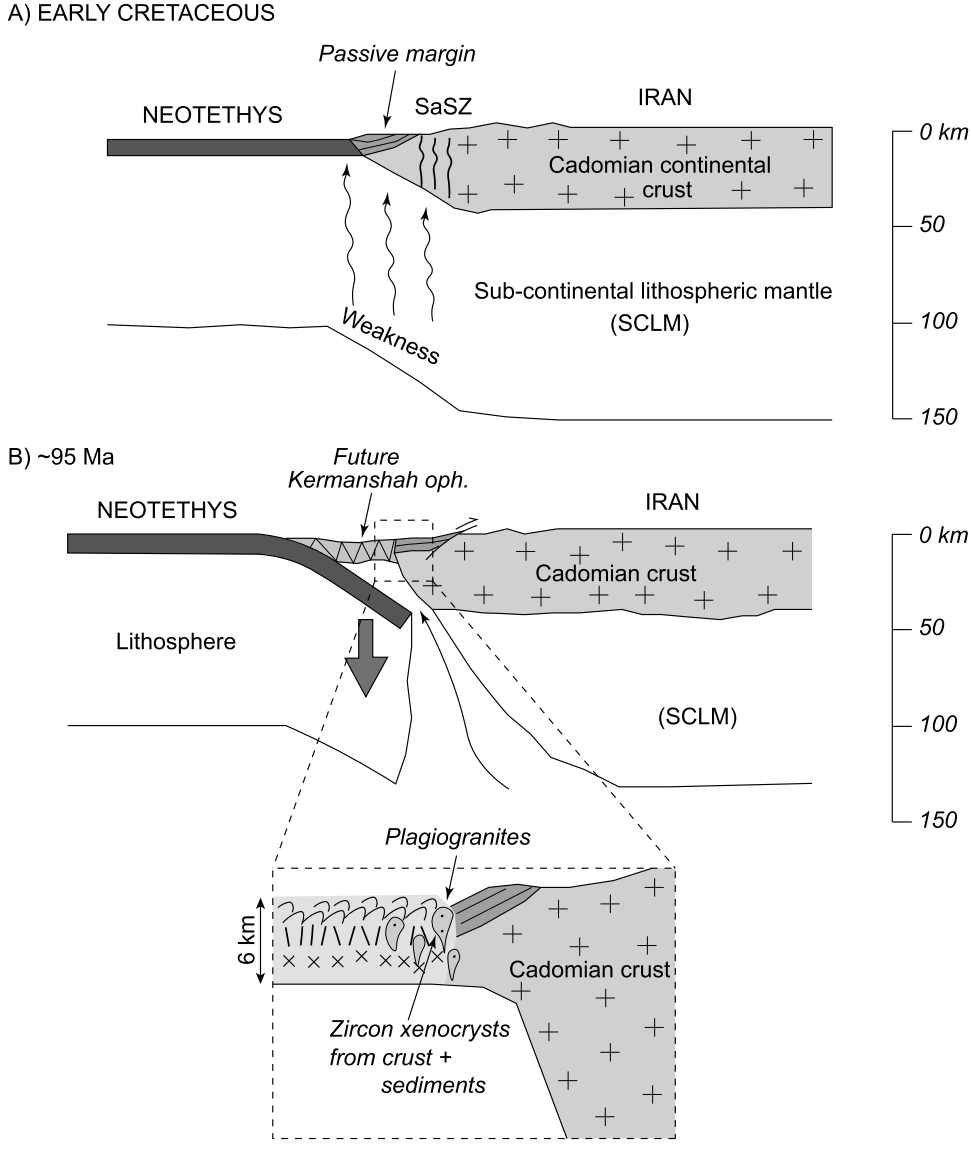

Figure 5. Schematic model explains the SI along the Iranian continental margin during late cretaceous which is presumed to be the fundamental mechanism for the concentration of the zircon xenocrysts in the kermanshah ophiolite.

ophiolitic plagiogranites include low-pressure fractional crystallization of hydrated basaltic melt (Amri *et al*. 1996) and late-stage products of silicate liquid immiscibility (Dixon and Rutherford 1979). Fluid-induced anatexis of mafic rocks, e.g. hornblende gabbros and/or amphibolites (Pedersen and Malpas 1984), in the roof zone of an axial magma chamber, is another mechanism for the formation of plagiogranites (Rollinson 2009). However, the lack of amphibolites in association with plagiogranites rule out anatexis of these rocks to produce Kermanshah plagiogranites. On the other hand, the absence of field evidence, as well as trace element patterns of plagiogranites and gabbros don't support wet anatexis of gabbros to generate the Kermnanshah plagiogranites. The plagiogranitic melts produced by hydrous partial melting of gabbros would have very low REE and TiO_2, because the compositionally refractory gabbroic rocks are depleted in REE and TiO_2 (e.g. Koepke *et al*. 2007).

The rare-earth and trace element patterns of plagiogranites are similar and broadly parallel to the Kermanshah lavas with Island-arc tholeiitic compositions. Therefore, fractional crystallization of the arc tholeiitic basaltic melts is possible to produce the Kermanshah plagiogranites. Assuming a density of hydrous basaltic (near MORB-like) melts in upper mantle of ~ 2.38 g-cm^{-3} (Bajgain *et al*. 2015) and the density of zircons as ~4.7 gcm^{-3} (Guo *et al*. 2020), it is difficult to understand how old zircons can be retained in a final fractionated melt and/or within melts from anatexis of hydrous gabbros. Therefore, our results suggest another related mechanism: coupled assimilation and fractional crystallization (AFC) involving mafic magmas intruding passive continental margin sediments.

Considering all these assumptions, we prefer to explain the presence of xenocrystic zircons in Kermanshah ophiolitic plagiogranites as due to the assimilation of Iranian continental crust and overlying sediments during subduction initiation of Neotethys, which fixes this at the margin of Iran during the Late Cretaceous, ~100-95 Ma (Figure 3).

7. Conclusions

Zircon xenocrysts from some plagiogranites in the 99–96 Ma Kermanshah ophiolite of SW Iran have U-Pb ages of Early Cretaceous (135–123 Ma), Jurassic-Triassic (250–155 Ma), Permian (290–255 Ma), Carboniferous-Devonian (421–312 Ma), Cadomian (625–526 Ma), Cryogenian-Tonian (929–652 Ma), Mesoproterozoic (1.5–1 Ga), Paleoproterozoic (2.5–1.6 Ga) and Meso-Archaean (~3 Ga). These zircon xenocrysts have εHf(t) values between +6.3 and – 21.6, corresponding to depleted mantle Hf model ages (T_{DM}) of 0.6 to 3.6 Ga. The age and Hf-isotope compositions of the zircon xenocrysts suggest their derivation from older magmatic and sedimentary rocks of the Iranian continental crust. The participation and assimilation of Iranian continental crust and sediments in Late Cretaceous ophiolites is best explained as a result of magmatism associated with subduction initiation beneath Iran along the SW Iran continental margin.

Acknowledgments

This study was funded by the "National Key Research and Development Program of China (2016YFE0203000)", "Chinese Academy of Sciences, President's International Fellowship Initiative (PIFI, 2019VCB0013)". This study used instrumentation funded by ARC LIEF and DEST Systemic Infrastructure Grants, Macquarie University, NCRIS AuScope and Industry. This is contribution 1697 from the ARC Centre of Excellence for Core to Crust Fluid Systems (http://www.ccfs.mq.edu.au), 1495 in the GEMOC Key Centre (http://www.gemoc.mq.edu.au), and 1681 from UTD Geosciences. All logistical support for the fieldwork came from Damghan University, Iran. We are very grateful to I. Monsef and H. Azizi for their constructive reviews of the manuscript. Editorial suggestions by S.A. Whattam are also appreciated.

Disclosure statement

No potential conflict of interest was reported by the author(s).

Funding

This work was supported by the National Key Research and Development Program of China [2016YFE0203000].

References

Agard, P., Omrani, J., Jolivet, L., and Mouthereau, F., 2005, Convergence history across Zagros (Iran): Constraints from collisional and earlier deformation: International Journal of Earth Sciences, 943, 401–419. 10.1007/s00531-005-0481-4

Ali, S.A., Buckman, S., Aswad, K.J., Jones, B.G., Ismail, S.A., and Nutman, A.P., 2013, The tectonic evolution of a Neo-Tethyan (Eocene-Oligocene) Island-arc (Walash and Naopurdan groups) in the Kurdistan region of the Northeast Iraqi Zagros Suture Zone: Island Arc, 221, 104–125. 10.1111/iar.12007

Amri, I., Benoit, M., and Ceuleneer, G., 1996, Tectonic setting for the genesis of oceanic plagiogranites: Evidence from a paleo-spreading structure in the Oman ophiolite: Earth and Planetary Science Letters, 1391–2, 177–194. 10.1016/0012-821X(95)00233-3

Ao, S., Xiao, W., Jafari, M.K., Talebian, M., Chen, L., Wan, B., Ji, W., and Zhang, Z., 2016, U–Pb zircon ages, field geology and geochemistry of the Kermanshah ophiolite (Iran): From

continental rifting at 79Ma to oceanic core complex at ca. 36Ma in the southern Neo-Tethys: Gondwana Research, 31, 305–318. 10.1016/j.gr.2015.01.014

Azizi, H., and Stern, R.J., 2019, Jurassic igneous rocks of the central Sanandaj–Sirjan zone (Iran) mark a propagating continental rift, not a magmatic arc: Terra Nova, 315, 415–423. 10.1111/ter.12404

Bajgain, S., Ghosh, D.B., and Karki, B.B., 2015, Structure and density of basaltic melts at mantle conditions from first-principles simulations: Nature Communications, 61, 8578. 10.1038/ncomms9578

Bindeman, I.N., and Melnik, O.E., 2016, Zircon survival, rebirth and recycling during crustal melting, magma crystallization, and mixing based on numerical modelling: Journal of Petrology, 573, 437–460. 10.1093/petrology/egw013

Blanco-Quintero, I.F., Gerya, T.V., Garcia-Casco, A., and Castro, A., 2011, Subduction of young oceanic plates: A numerical study with application to aborted thermal-chemical plumes: Geochemistry, Geophysics, Geosystems, 1210. 10.1029/2011GC003717

Braud, J., and Bellon, H., 1974. Données nouvelles sur le domaine métamorphique du Zagros (zone de Sanandaj–Sirjan) au niveau de Kermanshah–Hamadan (Iran): Nature âge et interprétation des séries métamorphiques et des intrusions; évolution structurale. Rapport Universite Paris-Sud, 1–20.

Chauvet, F., Lapierre, H., Maury, R.C., Bosch, D., Basile, C., Cotten, J., Brunet, P., and Campillo, S., 2011, Triassic alkaline magmatism of the hawasina nappes: post-breakup melting of the oman lithospheric mantle modified by the permian neotethyan plume: Lithos, 1221–2, 122–136. 10.1016/j.lithos.2010.12.006

Dilek, Y., and Furnes, H., 2014, Ophiolites and their origins: Elements, 10(2), 93–100. 10.2113/gselements.10.2.93

Dilek, Y., and Thy, P., 2009, Island arc tholeiite to boninitic melt evolution of the cretaceous kizildag (turkey) ophiolite: model for multi-stage early arc–forearc magmatism in tethyan subduction factories: Lithos, 1131–2, 68–87. 10.1016/j.lithos.2009.05.044

Dixon, S., and Rutherford, M., 1979, Plagiogranites as late-stage immiscible liquids in ophiolite and mid-ocean ridge suites: An experimental study: Earth and Planetary Science Letters, 451, 45–60. 10.1016/0012-821X(79)90106-7

Furnes, H., Dilek, Y., Zhao, G., Safonova, I., and Santosh, M., 2020, Geochemical characterization of ophiolites in the alpine-himalayan orogenic belt: magmatically and tectonically diverse evolution of the mesozoic neotethyan oceanic crust: Earth-Science Reviews, 208, 103258.

Gorczyk, W., Gerya, T.V., Connolly, J.A.D., and Yuen, D.A., 2007a, Growth and mixing dynamics of mantle wedge plumes: Geology, 357, 587–590. 10.1130/G23485A.1

Gorczyk, W., Willner, A.P., Gerya, T.V., Connolly, J.A.D., and Burg, J.-P., 2007b, Physical controls of magmatic productivity at pacific-type convergent margins: numerical modelling: Physics of the Earth and Planetary Interiors, 1631–4, 209–232. 10.1016/j.pepi.2007.05.010

Griffin, W.L., Afonso, J.C., Belousova, E.A., Gain, S.E., Gong, X.-H., Gonzalez-Jimenez, J.M., Howell, D., Huang, J.-X., McGowan, N., and Pearson, N.J., 2016, Mantle recycling: Transition zone metamorphism of Tibetan ophiolitic peridotites and its tectonic implications: Journal of Petrology, 574, 655–684. 10.1093/petrology/egw011

Griffin, W.L., Belousova, E.A., Shee, S.R., Pearson, N.J., and O'Reilly, S.Y., 2004, Archean crustal evolution in the northern Yilgarn Craton: U–Pb and Hf-isotope evidence from detrital zircons: Precambrian Research, 1313–4, 231–282. 10.1016/j.precamres.2003.12.011

Guo, S.-L., Chen, B.-L., and Durrani, S., 2020, Solid-state nuclear track detectors, handbook of radioactivity analysis, Academic Press, 307–407.

Harley, S.L., Kelly, N.M., and Möller, A., 2007, Zircon behaviour and the thermal histories of mountain chains: Elements, 31, 25–30. 10.2113/gselements.3.1.25

Honarmand, M., Li, X.-H., Nabatian, G., and Neubauer, F., 2017, In-situ zircon U-pb age and hf-o isotopic constraints on the origin of the hasan-robat a-type granite from sanandaj–Sirjan zone, Iran: Implications for reworking of cadomian arc igneous rocks: Mineralogy and Petrology, 1115, 659–675. 10.1007/s00710-016-0490-y

Ishikawa, T., Nagaishi, K., and Umino, S., 2002, Boninitic volcanism in the Oman ophiolite: Implications for thermal condition during transition from spreading ridge to arc: Geology, 30(10), 899–902. 10.1130/0091-7613(2002)030<0899:BVITOO>2.0.CO;2

Koepke, J., Berndt, J., Feig, S.T., and Holtz, F., 2007, The formation of SiO2-rich melts within the deep oceanic crust by hydrous partial melting of gabbros: Contributions to Mineralogy and Petrology, 1531, 67–84. 10.1007/s00410-006-0135-y

Lian, D., Yang, J., Dilek, Y., Wiedenbeck, M., Wu, W., and Rocholl, A., 2020, Precambrian zircons in chromitites of the cretaceous aladag ophiolite (Turkey) indicate deep crustal recycling in oceanic mantle: Precambrian Research, 350, 105838. 10.1016/j.precamres.2020.105838

Maffione, M., Hinsbergen, D.J.J., Gelder, G.I.N.O., Goes, F.C., and Morris, A., 2017, Kinematics of late cretaceous subduction initiation in the neo-tethys ocean reconstructed from ophiolites of Turkey, Cyprus, and Syria: Journal of Geophysical Research: Solid Earth, 1225, 3953–3976. 10.1002/2016JB013821

Malusà, M.G., Anfinson, O.A., Dafov, L.N., and Stockli, D.F., 2016, Tracking adria indentation beneath the alps by detrital zircon u-pb geochronology: implications for the oligocene–miocene dynamics of the Adriatic microplate: Geology, 442, 155–158. 10.1130/G37407.1

Marschall, H.R., and Schumacher, J.C., 2012, Arc magmas sourced from mélange diapirs in subduction zones: Nature Geoscience, 512, 862–867. 10.1038/ngeo1634

Mcdonough, W.F., and Sun, -S.-S., 1995, The composition of the earth: Chemical Geology, 120(3–4), 223–253. 10.1016/0009-2541(94)00140-4

McGowan, N.M., Griffin, W.L., González-Jiménez, J.M., Belousova, E., Afonso, J.C., Shi, R., McCammon, C.A., Pearson, N.J., and O'Reilly, S.Y., 2015, Tibetan chromitites: Excavating the slab graveyard: Geology, 432, 179–182. 10.1130/G36245.1

Moghadam, H.S., Li, Q.L., Griffin, W.L., Chiaradia, M., Hoernle, K., O'Reilly, S.Y., and Esmaeili, R., 2021b, The middle-late cretaceous zagros ophiolites, Iran: Linking of a 3000 km swath of subduction initiation fore-arc lithosphere from Troodos: Cyprus to Oman, GSA Bulletin.

Moghadam, H.S., Li, Q.-L., Griffin, W.L., Karsli, O., Santos, J.F., Ottley, C., Ghorbani, G., and O'Reilly, S.Y., 2020a, Tracking the birth and growth of cimmeria: geochronology and origins of intrusive rocks from nw Iran: Gondwana Research, 87, 188–206. 10.1016/j.gr.2020.06.012

Moghadam, H.S., Li, Q., Griffin, W., Stern, R., Santos, J., Lucci, F., Beyarslan, M., Ghorbani, G., Ravankhah, A., and Tilhac, R., 2021a, Prolonged magmatism and growth of the Iran-Anatolia Cadomian continental arc segment in Northern Gondwana: Lithos, 105940, 384.

Moghadam, H.S., and Stern, R.J., 2011, Geodynamic evolution of upper cretaceous zagros ophiolites: Formation of oceanic lithosphere above a nascent subduction zone: Geological Magazine, 1485–6, 762–801. 10.1017/S0016756811000410

Moghadam, H.S., and Stern, R.J., 2015, Ophiolites of Iran: Keys to understanding the tectonic evolution of SW Asia: (II) Mesozoic ophiolites: Journal of Asian Earth Sciences, 100, 31–59. 10.1016/j.jseaes.2014.12.016

Moghadam, H.S., Stern, R.J., Griffin, W., Khedr, M., Kirchenbaur, M., Ottley, C., Whattam, S., Kimura, J.-I., Ghorbani, G., and Gain, S., 2020b, Subduction initiation and back-arc opening north of Neo-Tethys: Evidence from the Late Cretaceous Torbat-e-Heydarieh ophiolite of NE Iran: Bulletin, 132, 1083–1105.

Monsef, I., Monsef, R., Mata, J., Zhang, Z.Y., Pirouz, M., Rezaeian, M., Esmaeili, R., and Xiao, W.J., 2018, Evidence for an early-MORB to fore-arc evolution within the zagros suture zone: constraints from zircon u-pb geochronology and geochemistry of the neyriz ophiolite (South Iran): Gondwana Research, 62, 287–305. 10.1016/j.gr.2018.03.002

Monsef, R., Monsef, I., and Rahgoshay, M., 2014, Geodynamic significance of the Janatabad peridotites and associated chromitites (S Iran): Implications for subduction initiation: Ofioliti, 39, 67–78.

Monsef, I., Rahgoshay, M., Pirouz, M., Chiaradia, M., Grégoire, M., and Ceuleneer, G., 2019, The eastern makran ophiolite (SE Iran): Evidence for a Late Cretaceous fore-arc oceanic crust: International Geology Review, 6111, 1313–1339. 10.1080/00206814.2018.1507764

Nouri, F., Azizi, H., Golonka, J., Asahara, Y., Orihashi, Y., Yamamoto, K., Tsuboi, M., and Anma, R., 2016, Age and petrogenesis of na-rich felsic rocks in western Iran: evidence for closure of the southern branch of the neo-tethys in the late cretaceous: Tectonophysics, 671, 151–172. 10.1016/j.tecto.2015.12.014

Pedersen, R.B., and Malpas, J., 1984, The origin of oceanic plagiogranites from the karmoy ophiolite, western Norway: Contributions to Mineralogy and Petrology, 881–2, 36–52. 10.1007/bf00371410

Peltonen, P., Mänttäri, I., Huhma, H., and Kontinen, A., 2003, Archean zircons from the mantle: The Jormua ophiolite revisited: Geology, 317, 645–648. 10.1130/0091-7613(2003)031<0645:AZFTMT>2.0.CO;2

Proenza, J., González-Jiménez, J.M., Garcia-Casco, A., Belousova, E., Griffin, W., Talavera, C., Rojas-Agramonte, Y., Aiglsperger, T., Navarro-Ciurana, D., and Pujol-Solà, N., 2018a, Cold plumes trigger contamination of oceanic mantle wedges with continental crust-derived sediments: Evidence from chromitite zircon grains of eastern Cuban ophiolites: Geoscience Frontiers, 96, 1921–1936. 10.1016/j.gsf.2017.12.005

Proenza, J.A., González-Jiménez, J.M., Garcia-Casco, A., Belousova, E., Griffin, W.L., Talavera, C., Rojas-Agramonte, Y., Aiglsperger, T., Navarro-Ciurana, D., Pujol-Solà, N., Gervilla, F., O'Reilly, S.Y., and Jacob, D.E., 2018b, Cold plumes trigger contamination of oceanic mantle wedges with continental crust-derived sediments: Evidence from chromitite zircon grains of eastern Cuban ophiolites: Geoscience Frontiers, 96, 1921–1936. 10.1016/j.gsf.2017.12.005

Rioux, M., Bowring, S., Kelemen, P., Gordon, S., Miller, R., and Dudas, F., 2013, Tectonic development of the Samail ophiolite: High-precision U-Pb zircon geochronology and Sm-Nd isotopic constraints on crustal growth and emplacement: Journal of Geophysical Research: Solid Earth, 1185, 2085–2101. 10.1002/jgrb.50139

Rioux, M., Garber, J., Bauer, A., Bowring, S., Searle, M., Kelemen, P., and Hacker, B., 2016, Synchronous formation of the metamorphic sole and igneous crust of the Semail ophiolite: New constraints on the tectonic evolution during ophiolite formation from high-precision U–Pb zircon geochronology: Earth and Planetary Science Letters, 451, 185–195. 10.1016/j.epsl.2016.06.051

Rojas-Agramonte, Y., Garcia-Casco, A., Kemp, A., Kroner, A., Proenza, J.A., Lazaro, C., and Liu, D.Y., 2016b, Recycling and transport of continental material through the mantle wedge above subduction zones: A Caribbean example: Earth and Planetary Science Letters, 436, 93–107. 10.1016/j.epsl.2015.11.040

Rojas-Agramonte, Y., Garcia-Casco, A., Kemp, A., Kröner, A., Proenza, J.A., Lázaro, C., and Liu, D., 2016a, Recycling and transport of continental material through the mantle wedge above subduction zones: A caribbean example: Earth and Planetary Science Letters, 436, 93–107. 10.1016/j.epsl.2015.11.040

Rojas-Agramonte, Y., Kaus, B., Piccolo, A., Williams, I., Gerdes, A., Wong, J., Xie, H., Buhre, S., Toulkeridis, T., and Montero, P., 2021, Asthenospheric zircon below Galápagos dates plume activity.

Rollinson, H., 2009, New models for the genesis of plagiogranites in the Oman ophiolite: Lithos, 1123–4, 603–614. 10.1016/j.lithos.2009.06.006

Saccani, E., Allahyari, K., Beccaluva, L., and Bianchini, G., 2013, Geochemistry and petrology of the kermanshah ophiolites (Iran): implication for the interaction between passive rifting, oceanic accretion, and OIB-type components in the Southern Neo-Tethys Ocean: Gondwana Research, 241, 392–411. 10.1016/j.gr.2012.10.009

Savelieva, G., Sharaskin, A.Y., Saveliev, A., Spadea, P., and Gaggero, L., 1997, Ophiolites of the southern uralides adjacent to the East European continental margin: Tectonophysics, 2761–4, 117–137. 10.1016/S0040-1951(97)00053-X

Searle, M.P., and Malpas, J., 1980, Structure and metamorphism of rocks beneath the Semail ophiolite of Oman and their significance in ophiolite obduction: Transactions of the Royal Society of Edinburgh: Earth Sciences, 714, 247–262. 10.1017/S0263593300013614

Sepidbar, F., Lucci, F., Biabangard, H., Zaki Khedr, M., and Jiantang, P., 2020, Geochemistry and tectonic significance of the Fannuj-Maskutan SSZ-type ophiolite (Inner Makran, SE Iran): International Geology Review, 6216, 2077–2104. 10.1080/00206814.2020.1753118

Smyth, H., Hamilton, P., Hall, R., and Kinny, P., 2007, The deep crust beneath Island arcs: Inherited zircons reveal a Gondwana continental fragment beneath East Java, Indonesia: Earth and Planetary Science Letters, 2581–2, 269–282. 10.1016/j.epsl.2007.03.044

Spandler, C., and Pirard, C., 2013, Element recycling from subducting slabs to arc crust: A review: Lithos, 170-171, 208–223. 10.1016/j.lithos.2013.02.016

Stern, R.J., Ali, K.A., Liegeois, J.P., Johnson, P.R., Kozdroj, W., and Kattan, F.H., 2010, Distribution and significance of pre-neoproterozoic zircons in juvenile neoproterozoic igneous rocks of the Arabian-Nubian Shield: American Journal of Science, 310(9), 791–811. 10.2475/09.2010.02

Stern, R.J., and Bloomer, S.H., 1992, Subduction zone infancy: examples from the eocene izu-bonin-mariana and jurassic California arcs: Geological Society of America Bulletin, 10412, 1621–1636. 10.1130/0016-7606(1992)104<1621:SZIEFT>2.3.CO;2

Stern, R.J., and Gerya, T., 2018, Subduction initiation in nature and models: A review: Tectonophysics, 746, 173–198. 10.1016/j.tecto.2017.10.014

Stern, R.J., Reagan, M., Ishizuka, O., Ohara, Y., and Whattam, S., 2012, To understand subduction initiation, study forearc crust: To understand forearc crust, study ophiolites: Lithosphere, 46, 469–483. 10.1130/L183.1

Torró, L., Proenza, J.A., Rojas-Agramonte, Y., Garcia-Casco, A., Yang, J.-H., and Yang, Y.-H., 2018, Recycling in the subduction factory: archaean to permian zircons in the oceanic cretaceous caribbean Island-arc (Hispaniola): Gondwana Research, 54, 23–37. 10.1016/j.gr.2017.09.010

Vermeesch, P., 2018, IsoplotR: A free and open toolbox for geochronology: Geoscience Frontiers, 95, 1479–1493. 10.1016/j.gsf.2018.04.001

Warren, C.J., Parrish, R.R., Waters, D.J., and Searle, M.P., 2005, Dating the geologic history of Oman's Semail ophiolite: Insights from U-Pb geochronology: Contributions to Mineralogy and Petrology, 150(4), 403–422. 10.1007/s00410-005-0028-5

Whattam, S.A., Malpas, J., Smith, I.E.M., and Ali, J.R., 2006, Link between SSZ ophiolite formation, emplacement and arc inception, Northland, New Zealand: U–Pb SHRIMP constraints; Cenozoic SW Pacific tectonic implications: Earth and Planetary Science Letters, 250(3–4), 606–632. 10.1016/j.epsl.2006.07.047

Whetten, J.T., Zartman, R.E., Blakely, R.J., and Jones, D.L., 1980, Allochthonous jurassic ophiolite in northwest Washington: Geological Society of America Bulletin, 916, 359–368. 10.1130/0016-7606(1980)91<359:AJOINW>2.0.CO;2

Wrobel-Daveau, J.-C., Ringenbach, J.-C., Tavakoli, S., Ruiz, G.M. H., Masse, P., and de Lamotte, D.F., 2010, الجيولوجيا البنيوية لمنطقة كرمنشاه (إيران) على حدود الصفيحة العربية في الزاقروس: Arabian Journal of Geosciences, 34, 499–513. 10.1007/s12517-010-0209-z

Yamamoto, S., Komiya, T., Yamamoto, H., Kaneko, Y., Terabayashi, M., Katayama, I., Iizuka, T., Maruyama, S., Yang, J., and Kon, Y., 2013a, Recycled crustal zircons from podiform chromitites in the Luobusa ophiolite, southern Tibet: Island Arc, 221, 89–103. 10.1111/iar.12011

Yamamoto, S., Komiya, T., Yamamoto, H., Kaneko, Y., Terabayashi, M., Katayama, I., Iizuka, T., Maruyama, S., Yang, J.S., Kon, Y., and Hirata, T., 2013b, Recycled crustal zircons from podiform chromitites in the Luobusa ophiolite, southern Tibet: Island Arc, 221, 89–103. 10.1111/iar.12011

Yang, J.S., Meng, F.C., Xu, X.Z., Robinson, P.T., Dilek, Y., Makeyev, A.B., Wirth, R., Wiedenbeck, M., and Cliff, J., 2015, Diamonds, native elements and metal alloys from chromitites of the Ray-Iz ophiolite of the Polar Urals: Gondwana Research, 272, 459–485. 10.1016/j.gr.2014.07.004